Zagazig University Medical Journal
www.zumj.journals.ekb.eg
https://doi.org/10.21608/zumj.2025.417993.4133 Volume 31, Issue 11 November. 2025
Manuscript ID:ZUMJ-2508-4133
DOI:10.21608/zumj.2025.417993.4133

ORIGINAL ARTICLE

Comparison of Steroid and Botulinum Toxin Type A Monotherapy with Combination Therapy for Human Hypertrophic Scars in an Animal Model

Rafaat Abd-allatif Anany, Mohamed Ahmed Mohamed Ahmed Elayady*, Ahmed Mohamed Ali

Department of Plastic & Reconstructive Surgery, Faculty of Medicine, Zagazig University, Egypt

***Corresponding author:**
Mohamed Ahmed Mohamed Ahmed Elayady
E-mail:
moelayady@gmail.com

Submit Date: 27-08-2025
Accept Date: 26-09-2025

ABSTRACT

Background: Hypertrophic scars are a challenging complication of wound healing, characterized by excessive fibroblast proliferation, collagen deposition, and persistent inflammation. Current intralesional therapies, such as corticosteroids, show partial efficacy but are often associated with adverse effects. Botulinum toxin type A (BoNT-A) has emerged as a potential therapeutic option, and its combination with corticosteroids may provide a synergistic effect. This study aimed to evaluate and compare the histopathological effects of intralesional triamcinolone acetonide, botulinum toxin type A, and their combination in hypertophic scar in an animal model.

Methods: A total of forty scar samples were randomly assigned into four groups: control with saline, triamcinolone acetonide, BoNT-A, and a combined regimen of both agents. Histopathological assessment was performed after four weeks, focusing on inflammatory activity, fibroblast proliferation, collagen deposition, necrosis, and tissue reconstruction.

Results: The control group exhibited persistent fibroblast activity and dense collagen fibers, consistent with the natural progression of untreated hypertrophic scars. The triamcinolone group showed reduced fibroblast activity but was associated with acute inflammation, epidermal necrosis, and focal collagen deposition. The BoNT-A group demonstrated decreased vascularization, suppressed fibroblast activity, partially organized collagen fibers, and gradual tissue reconstruction. The combination therapy group yielded the most favorable outcomes, with near-complete dermo-epidermal reconstruction, orderly collagen deposition, minimal necrosis, and resolution of persistent inflammation. **Conclusion:** Both triamcinolone and BoNT-A demonstrated efficacy in reducing hypertrophic scar features; however, their combination produced superior histopathological outcomes, reflecting a synergistic therapeutic effect. These findings highlight the potential of combined triamcinolone and BoNT-A therapy as a promising multimodal approach for hypertrophic scar management, warranting further clinical validation in human studies.

Keywords: Hypertrophic scar; Triamcinolone acetonide; Botulinum toxin type A; Combination therapy; Fibroblast proliferation

INTRODUCTION

Hypertrophic scarring remains a major clinical challenge following deep dermal burns and other delayed-healing injuries. Scars typically form within weeks after injury, and evidence suggests that wounds requiring more than three weeks to heal have a markedly increased risk of developing hypertrophic scars [1]. These scars are characterized by abnormal collagen deposition and dysregulated fibroblast activity, which frequently result in functional impairment, pain, pruritus, and cosmetic disfigurement.

Several therapeutic agents have been investigated for hypertrophic scar management, including corticosteroids, 5-fluorouracil, and interferons, delivered

primarily via intralesional injection. However, the variability in clinical response and the potential for adverse effects such as skin atrophy and hypopigmentation pose significant limitations to their use [2]. Currently, intralesional corticosteroids remain the most widely accepted treatment option. Their efficacy is attributed to multiple mechanisms, including increased fibroblast apoptosis, enhanced collagenase production, and suppression of fibroblast proliferation. Accordingly, the International Advisory Panel on Scar Management continues to recommend intralesional steroid injections for the treatment of both keloids and hypertrophic scars [3].

Botulinum toxin type A (BTX-A), a neurotoxin derived from *Clostridium botulinum*, has gained attention as a potential alternative or adjunctive therapy. Beyond its established role in aesthetic medicine, BTX-A has shown promise in scar modulation. Experimental studies have demonstrated that BTX-A reduces fibroblast proliferation, alters cell cycle distribution, and downregulates transforming growth factor-β1 (TGF-β1) expression in fibroblasts derived from hypertrophic scars [4]. Additionally, by reducing muscle contraction during wound healing, BTX-A minimizes wound tension, thereby decreasing the risk of hypertrophic scar formation.

Aim of the work:

This study aimed to evaluate the most effective minimally invasive approach for the treatment of human hypertrophic scars by comparing the therapeutic outcomes of intralesional corticosteroid monotherapy, botulinum toxin type A monotherapy, and their combined use in an established animal model implanted with human scar tissue.

METHODS

This prospective experimental study was conducted at the Zagazig University Microsurgery Center (ZUMC), Plastic and Reconstructive Surgery Department, Faculty of Medicine, Zagazig University, Egypt, between September 2023 and September 2024. The study protocol was reviewed and approved by the Institutional Review Board for human tissue research (ZU-IRB# 11132-24/9-2023) and the Institutional Animal Care and Use Committee (ZU-IACUC/3/F/268/2023). All procedures were performed in accordance with institutional ethical standards, the principles of the Declaration of Helsinki, and the European guidelines for the care and use of laboratory animals.

Sample size:

Experimental study on 40 male albino rats. Assuming that scar weight reduction was 5% vs 50% in control vs Botox group. At 80% power and 95% CI, the estimated sample will be 40 rats, 10 rats in each group.

Eligibility Criteria (Human Participants): The inclusion criteria included patients who provided informed consent and agreed to participate, those with post-burn hypertrophic scars, and those undergoing either complete excision and coverage or serial excision of the scars. Additionally, patients who underwent these procedures without intraoperative complications and whose excised scars were processed and implanted within 120 minutes were included. Exclusion criteria consisted of patients who refused participation, those who experienced intraoperative complications during the excision and coverage procedures, and patients with medical conditions such as liver disease or immunological disorders that could potentially affect the wound healing process. Furthermore, patients undergoing immunosuppressive therapy, those diagnosed with malignancies (e.g., leukemia), and those for whom the processing and implantation time exceeded 120 minutes were excluded from the study.

Eligibility Criteria (Animal Subjects): The study included only male albino rats with an average weight ranging from 200 to 350 grams. All rats received appropriate anesthesia, administered intraperitoneally as ketamine at a dose of 0.08–0.09 mg per gram of body weight, during all surgical procedures. Only rats that survived for at least four weeks following the implantation procedure were included in the study. Female albino rats and other animal species, as well as rats with a weight outside the specified range (i.e., less than 200 grams or greater than 350 grams), were excluded. Additionally, rats

that experienced complications during the procedure, such as necrosis or infection at the incision site, or those that suffered graft loss, were excluded. Rats with known medical conditions that could impair wound healing, as well as rats that did not survive for at least four weeks post-implantation, were also excluded from the study

Animals

The experimental work included forty-nine young adult male Sprague-Dawley rats weighing between 150 and 300 grams. All animals were obtained from a controlled laboratory environment to minimize variability and were handled ethically throughout the study. Nine animals died before completion of the experimental period, leaving forty survivors for the final analysis.

Human Scar Specimens

Hypertrophic scar fragments were obtained from surgically treated burn patients. The excised tissues were collected in antiseptic flasks, hydrated in saline solution, and processed within two hours of harvest to ensure viability. Each scar fragment was trimmed into standardized specimens measuring approximately 1 × 1 cm before implantation.

Surgical Procedure

The rats were anesthetized with an intraperitoneal injection of a ketamine–xylazine cocktail (25mg ketamine + 10mg xylazine per mL) at a dose of 0.1mL/100g body weight. After anesthesia, the dorsal surface of each rat was shaved and sterilized with 10% povidone-iodine solution. A linear incision was made midway between the spine and the limb using a no. 15 surgical blade. Through blunt dissection with scissors, a subcutaneous pocket was created to accommodate the scar implant. Each specimen was then secured in the pocket, and the incision was closed with absorbable sutures (Fig. 1).

Experimental Groups

The implanted specimens were randomly assigned to four treatment groups. **Group A (Control group)** received intralesional injections of 0.9% normal saline (0.05 mL/g). **Group B (Steroid group)** was treated with triamcinolone acetonide (0.05 mL/g; 40 mg/mL suspension). **Group C (Botulinum toxin group)** received purified botulinum toxin type A (0.05 mL/g; 100 U/vial, diluted with 2.5 mL normal saline to achieve 40 U/mL). **Group D (Combination group)** received a mixture of triamcinolone acetonide (0.025 mL/g) and botulinum toxin type A (0.025 mL/g) using the same dilution.

Implantation Procedure

Following intralesional injection with the assigned drug, each human hypertrophic scar specimen was implanted subcutaneously into the dorsal region of the rats according to its designated group. Group A (Control) specimens were implanted at the midpoint between the left lower limb and the back, Group B (Steroid) specimens at the midpoint between the right lower limb and the back, Group C (Botulinum toxin) specimens at the midpoint between the right upper limb and the back, and Group D (Combination) specimens at the midpoint between the left upper limb and the back. After implantation, the skin was closed with interrupted 4-0 polypropylene sutures, and the incision site was sterilized with 10% povidone-iodine solution (Figure 2A, B, C).

Postoperative Care and Follow-Up

All rats were closely monitored throughout the perioperative period. Each animal was housed individually in a separate cage with free access to food and water. During the first postoperative week, daily assessments were performed to monitor feeding, general health, wound condition, and to provide local wound care and antibiotic coverage. Thereafter, follow-up was conducted every three days until the end of the 4-week experimental period. Systemic antibiotic prophylaxis was given only for 7 days in the form of tetracycline administered orally in drinking water at a dose of 0.8 mg/100 g rat body weight per 24 hours. After complete wound healing and closure, sutures were removed, and the rats were transferred to large communal cages approximately 4 weeks postoperatively.

Specimen Harvest and Histological Processing

At the end of the 4-week follow-up period, all surviving rats were anesthetized following the

same protocol used at the beginning of the study. Implanted specimens were carefully extracted from the dorsal subcutaneous pockets and immediately fixed in 10% buffered formalin.

Formalin-preserved scar tissues underwent automated tissue processing. The protocol included a two-step fixation and dehydration process: immersion in 10% buffered formalin for 48 hours, followed by rinsing in distilled water for 30 minutes. Dehydration was then carried out using a graded alcohol series (70% for 120 minutes, 90% for 90 minutes, and two cycles of absolute alcohol for 60 minutes each). This was followed by clearing in xylene, starting with a mixture of 50% alcohol and 50% xylene for 60 minutes, and then pure xylene for 90 minutes. Samples were subsequently impregnated with molten paraffin wax, embedded, and blocked out.

Paraffin sections of 4–5 μm thickness were stained with hematoxylin and eosin (H&E) according to standard protocols [5]. Histological evaluation focused on fibroblast activity, collagen fiber arrangement, inflammatory infiltration, degeneration, apoptosis, necrosis, and other pathological alterations.

Statistical analysis

Data were analyzed using the Statistical Package for Social Sciences (SPSS, version 24). Qualitative variables were summarized as frequencies and percentages, while quantitative variables were expressed as mean ± standard deviation (SD). Comparisons among more than two groups were performed using one-way analysis of variance (ANOVA) for normally distributed data. A *p*-value less than 0.05 was considered statistically significant, values below 0.001 were regarded as highly significant, whereas values greater than 0.05 were considered not significant.

RESULTS

The histopathological evaluation of the studied groups demonstrated distinct differences in inflammatory response, tissue degeneration, necrosis, fibroblast activity, and tissue reconstruction (table 1). **Inflammatory Process**: In Group A and Group D, all samples (100%) were free from any inflammatory process. In contrast, all samples (100%) in Group B exhibited an existing inflammatory process, while Group C showed remnants of inflammatory cells in all samples (100%). **Tissue Degeneration**: All samples (100%) in Group A showed no evidence of tissue degeneration. Conversely, all samples (100%) in Group B demonstrated tissue degeneration. In Group C, all samples (100%) exhibited destruction of both the epidermis and dermis, while Group D displayed only minimal tissue degeneration (100%). **Tissue Necrosis**: No tissue necrosis was observed in any samples from Group A (100%). In Group B, all samples (100%) displayed tissue necrosis specifically in epidermal cells. Group C samples (100%) showed tissue necrosis only in a few cases of caseated material, whereas Group D exhibited very limited tissue necrosis, with the affected material in the process of being cleared. **Fibroblast Activity**: In Group A, there were no changes in fibroblast activity across all samples (100%). In Group B and Group C, all samples (100%) showed decreased fibroblast activity. However, in Group D, all samples (100%) exhibited decreased fibroblast activity with mild collagen deposition, associated with new vascularization. **Tissue Reconstruction**: In Group A, no tissue reconstruction was observed in any of the samples (100%). In Group B, a small focal area with new collagen fibers was observed in all samples (100%). Group C showed gradual tissue reconstruction in all samples (100%), while Group D exhibited near-complete reconstruction of both the dermis and epidermis (100%).

In **Group A (control, saline-injected scars)**, sections of the saline injected control scar tissue showed elevated levels of fibroblasts and high density of collagen fibers, normal covering keratinized epidermis and underlying normally vascularized with regular structurally distributed dermis and hypodermis free of any inflammatory cellular infiltrate, tissue degeneration, necrosis or pyo-granulomatous reaction (Fig. 3).

In **Group B (Triamcinolone acetonide-injected scars)**, histological examination of the cortisone-treated group revealed acute inflammation process and total necrosis of the epidermal cells. PMNL were focally and

diffusely distributed and infiltrated the epidermis, dermal and hypodermal tissue, accompanied with partial tissue necrosis and liquefaction, there was an increase in the dermal vascularization. Fibroblast activity in the triamcinolone-treated group was significantly decreased, the dermis contained an irregularly configurated, extracellular matrix devoid of sizable amount of collagen, which can be confirmed by Masson trichrome stain. Only a small focal area had the new collagen fibers and granulation tissue formation, suggesting limited tissue reconstruction. Skin appendages were completely necrotized and disappeared (Fig. 4a, b).

In **Group C (Botulinum toxin type A-injected scars)**, histological examination of the botulinum toxin type A (BoNT-A) group revealed decreased fibroblast activity, low dermal vascularization and a decreased quantity of partially organized collagen deposition which suggests gradual tissue reconstruction. In a few cases dried caseated materials were seen in the healing process of the previously markedly inflamed, destructed epidermal and dermal tissues, with gradual tissue reconstruction (Fig. 5).

In **Group D (Combined Triamcinolone acetonide and Botulinum toxin type A-injected scars)**, the combination therapy group demonstrated decreased fibroblast activity with mild to moderate, orderly organized collagen deposition. Histological analysis revealed near-complete reconstruction of dermal and epidermal tissue, with collagen fibers arranged in a more structured and aligned manner, associated with new vascularization, free of any inflammatory process, a part of a very few amounts of dried necrotized materials, in their way to be washed out with the healing process and the gradual tissue remodeling and re-construction (Fig. 6).

Tables (1): Combined description of histopathological findings in studied groups.

		Groups							
		Group A (n = 10)		Group B (n = 10)		Group C (n = 10)		Group D (n = 10)	
Inflammatory process	Free	10	100%	0	0%	0	0%	10	100%
	Existing inflammatory process	0	0%	10	100%	0	0%	0	0%
	Remnants of inflammatory cells	0	0%	0	0%	10	100%	0	0%
Tissue Degeneration	None	10	100%	0	0%	0	0%	0	0%
	Yes	0	0%	10	100%	0	0%	0	0%
	Destructed Epidermis + Dermis	0	0%	0	0%	10	100%	0	0%
	Very few	0	0%	0	0%	0	0%	10	100%
Tissue necrosis	No	10	100%	0	0%	0	0%	0	0%
	Yes, in epidermal cells	0	0%	10	100%	0	0%	0	0%
	Only in a few cases of caseated material	0	0%	0	0%	10	100%	0	0%
	Very few (in their way to be washed out)	0	0%	0	0%	0	0%	10	100%
Past	No change	10	100%	0	0%	0	0%	0	0%

		Groups							
		Group A (n = 10)		Group B (n = 10)		Group C (n = 10)		Group D (n = 10)	
	Decreased	0	0%	10	100%	10	100%	0	0%
	Decreased (Mild collagen deposition due to new vascularization)	0	0%	0	0%	0	0%	10	100%
Tissue reconstruction	No	10	100%	0	0%	0	0%	0	0%
	Small Focal Area showed new collagen fibers	0	0%	10	100%	0	0%	0	0%
	Gradual Tissue reconstruction	0	0%	0	0%	10	100%	0	0%
	Near complete reconstruction of Dermis and epidermis	0	0%	0	0%	0	0%	10	100%

A

B

C

D

Figure 1: (A) shows the incision site after preparation of the rat's back, (B) & (C) demonstrates hypertrophic scar measurement while (D) shows a picture of the specimen**.**

Figure 2: (A) shows the incision site before placing the specimen in a subcutaneous pocket while (B) highlights the incision site after placing the specimen in a subcutaneous pocket. (C) a different site for specimen placement highlighting how different specimens are implanted in different areas for identification.

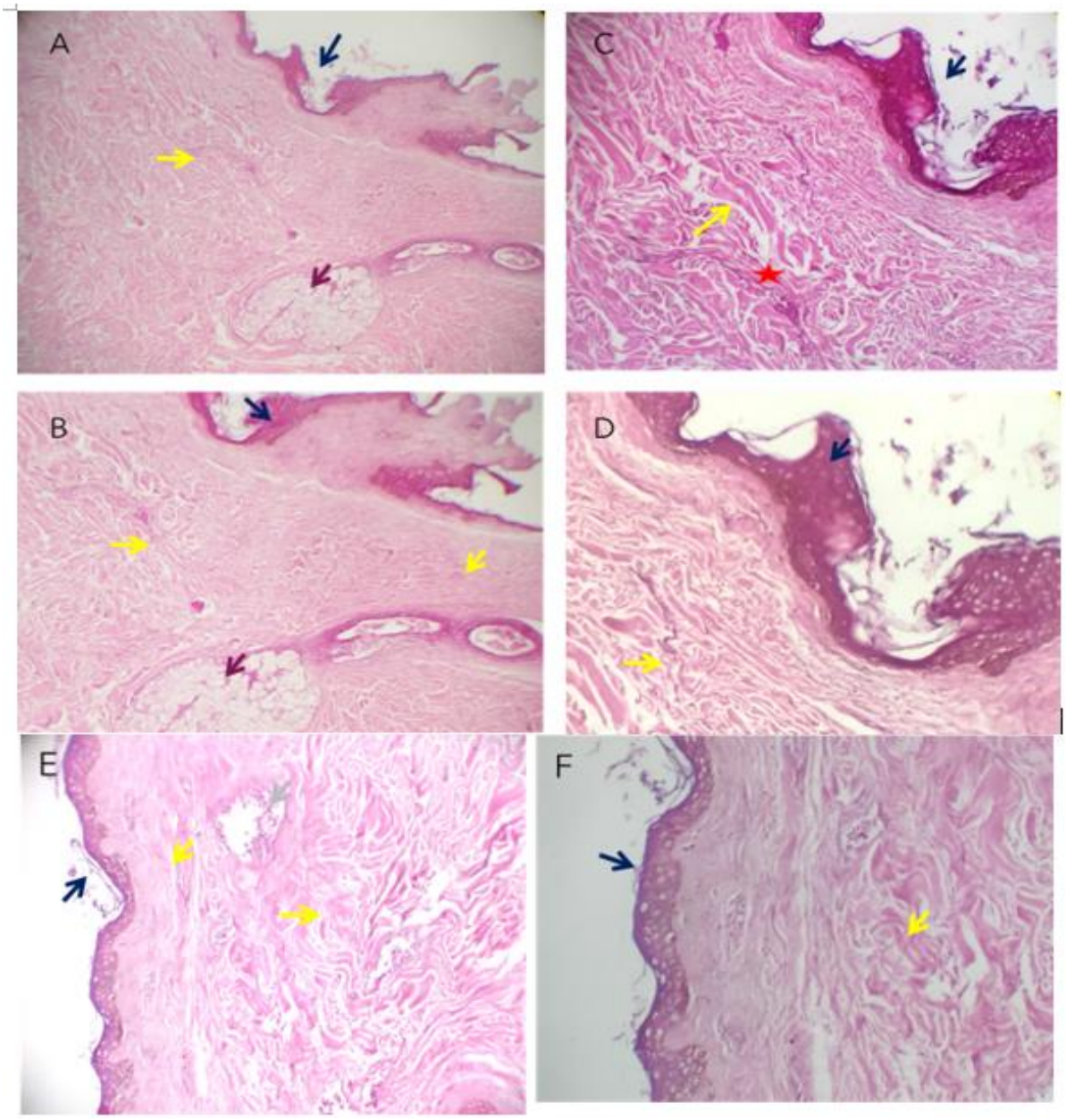

Figure 3: (A) and (B) show photomicrographs from the saline injected group stained with H&E at 100x and 400x magnification respectively, displaying elevated fibroblast activity with a high density of collagen fibers, a normal keratinized epidermis (dark blue arrows) with no inflammation or necrosis, indicating

hypertrophic scar persistence, (C) and (D) show photomicrographs at 100x and 400x magnification respectively, focusing on the epidermal-dermal junction and detailing the extracellular matrix with elevated fibroblast activity, dense collagen fibers and regular vascularization (red asterisk) in the dermis and hypodermis (yellow) and no signs of tissue degeneration or pyogranulomatous reaction while (E) and (F) show photomicrographs at 100x and 400x respectively, illustrating elevated fibroblast activity with well-organized collagen fibers in the hypodermis, consistent with untreated hypertrophic scar characteristics.

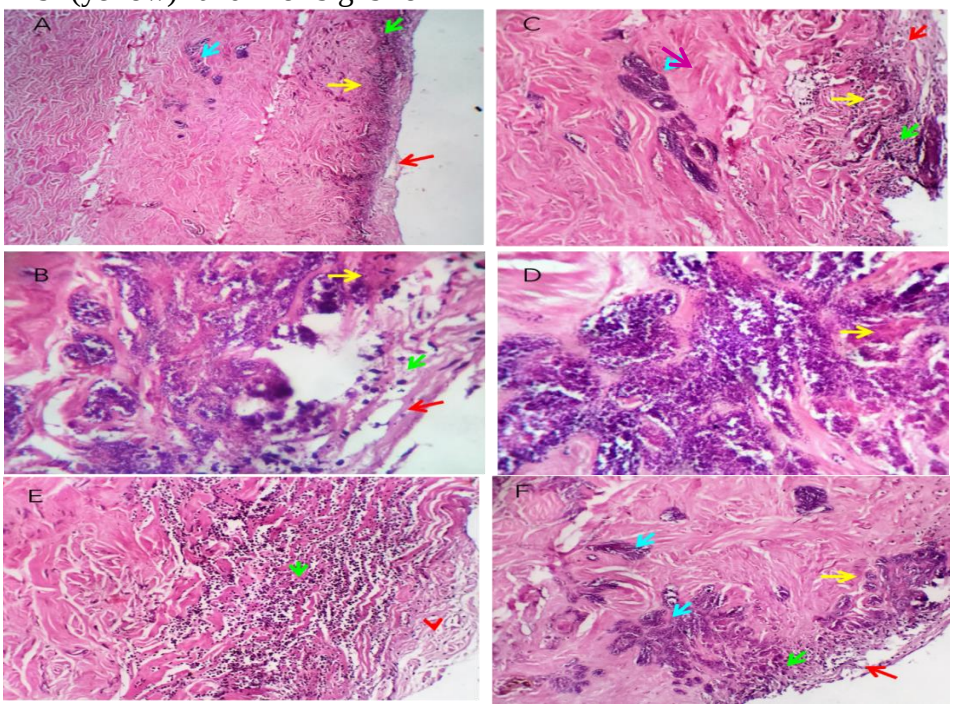

Figure 4a: Photomicrographs from Triamcinolone acetonide scar injected group stained with H&E in which (A) and (B) at 100x and 400x magnification respectively show decreased fibroblast activity with an irregular extracellular matrix lacking substantial collagen, accompanied by acute inflammation, total epidermal necrosis (red arrows), and diffuse polymorphonuclear leukocyte (PMNL) infiltration (green arrow) in the epidermis and dermis, (C) at 100x magnification shows decreased fibroblast activity with sparse collagen, focal areas of liquefaction necrosis (yellow arrows), and increased dermal vascularization (purple arrow), with no visible skin appendages due to complete necrosis, (D) at 400x magnification highlights a focal area of liquefaction necrosis (yellow arrow) while (E) and (F) illustrate decreased fibroblast activity in the hypodermis with minimal collagen, ongoing inflammation, and focal liquefaction necrosis, reflecting triamcinolone's suppressive impact on collagen synthesis.

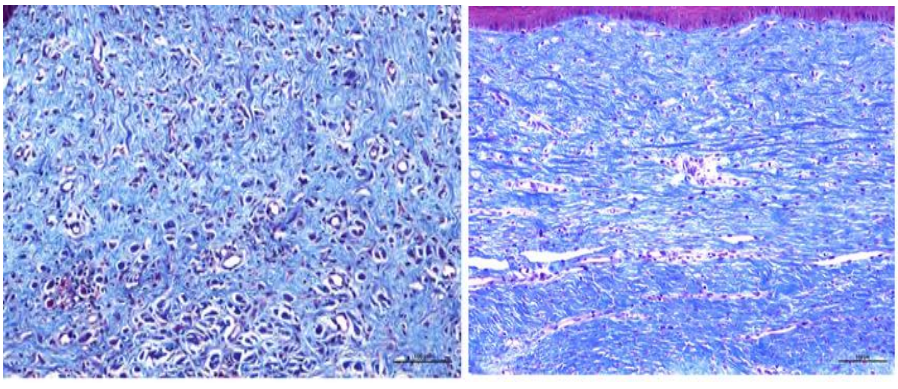

A **B**

Figure 4b: (G) shows a photomicrograph of saline-injected control scar tissue stained with Masson trichrome, displaying robust collagen deposition with a high density of tightly packed collagen fibers stained blue, indicative of elevated fibroblast activity typical of untreated hypertrophic scars while (H) shows a photomicrograph of triamcinolone acetonide-injected scar tissue, stained with Masson trichrome, revealing sparse collagen deposition with minimal blue-stained collagen fibers, except for a small focal area of new collagen, highlighting significantly reduced fibroblast activity due to triamcinolone's suppressive effect.

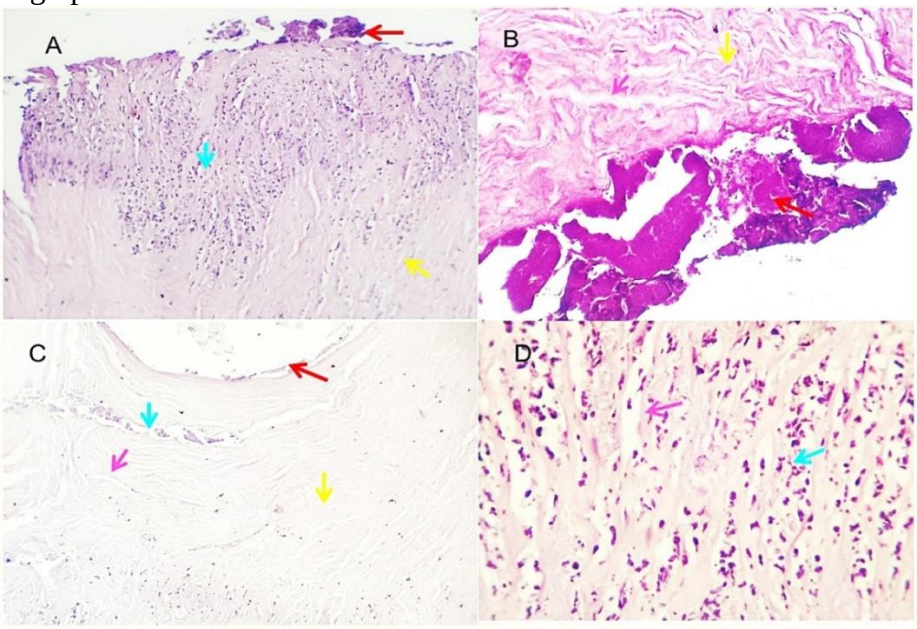

Figure 5: Photomicrographs from Botulinum toxin type A scar injected group stained with H&E in which (A) and (B) at 100x and 400x magnification respectively indicate the healing process of previously markedly inflamed, destructed epidermal and dermal tissues with gradual tissue reconstruction (red arrow), (C) at 100x magnification displays decreased fibroblast activity with low dermal vascularization (purple arrow) and a reduced quantity of partially organized collagen deposition (yellow arrows), alongside remnants of inflammatory cellular infiltrates (light blue arrows) indicating a healing process while (D) at 400x magnification highlights decreased fibroblast activity in the hypodermis with sparse collagen deposition and remnants of inflammatory infiltrates.

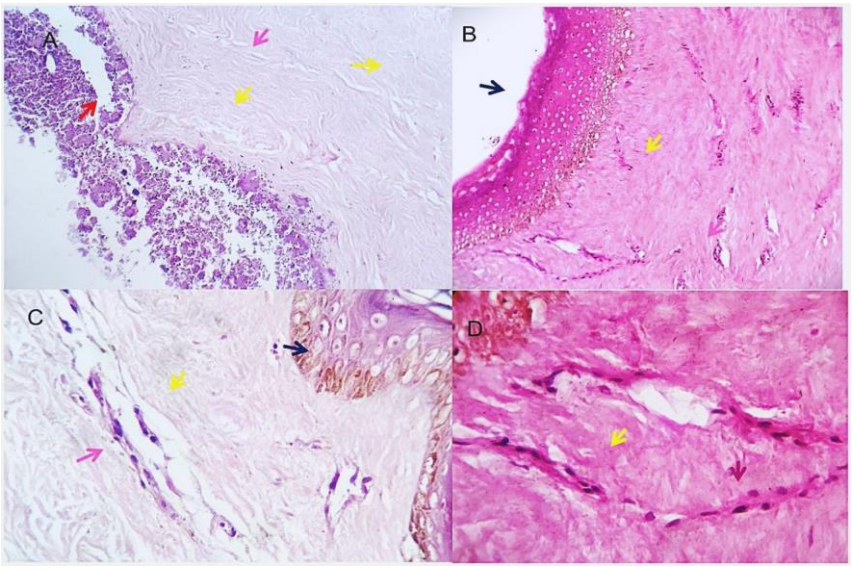

Figure 6: Photomicrographs from Triamcinolone acetonide and Botulinum toxin type A injected scars group stained with H&E in which (A) at 100x magnification shows decreased fibroblast activity with mild to moderate, orderly organized collagen deposition (yellow arrows) alongside new vascularization, with minimal dried necrotized material (red arrow) indicating ongoing healing, (B) and (C) at 100x and 400x magnification respectively show near-complete reconstruction of dermal and epidermal tissue (dark blue arrows) and new vascularization (purple arrows), while (D) at 400x magnification highlights a part of a very few amount of dried necrotized materials(red arrow) in their way to be washed out with the healing process and gradual tissue remodeling and reconstruction.

DISCUSSION

The control group (Group A), treated with saline, exhibited persistent high fibroblast activity and dense collagen deposition, consistent with the natural progression of hypertrophic scars. This aligns with prior research indicating that untreated hypertrophic scars maintain elevated fibroblast proliferation and collagen synthesis, contributing to scar hypertrophy [6]. The absence of tissue reconstruction in this group underscores the need for active intervention to modulate scar formation.

In Group B, treated with triamcinolone acetonide, histological analysis revealed acute inflammation, epidermal necrosis, and reduced collagen deposition, with only focal areas of new collagen fibers. These findings are consistent with the known mechanisms of corticosteroids, which suppress inflammation, reduce fibroblast proliferation, enhance collagenase production, and promote fibroblast apoptosis [7,8].

However, the observed tissue necrosis and persistent inflammation suggest potential limitations, such as tissue damage and delayed healing, which are well-documented side effects of corticosteroid injections, including skin atrophy and telangiectasia [9].

Group C, treated with BoNT-A, demonstrated reduced dermal vascularization, decreased collagen deposition, and gradual tissue reconstruction, with remnants of inflammatory cells and caseated material. BoNT-A's mechanism involves reducing mechanical tension by inhibiting muscle contraction, which mitigates scar widening and hypertrophy [10]. Additionally, BoNT-A suppresses fibroblast proliferation and downregulates transforming growth factor-beta 1 (TGF-β1), a key mediator of fibrosis [11,12]. These effects align with clinical studies showing improved scar aesthetics with BoNT-A, particularly in high-tension areas [13,14]. However, the presence of residual inflammatory cells suggests that BoNT-A alone may not fully resolve the inflammatory component of hypertrophic scarring.

The combination therapy in Group D (triamcinolone acetonide and BoNT-A) yielded the most promising results, with near-complete reconstruction of dermal and epidermal tissue, orderly collagen deposition, new vascularization, and minimal inflammation or necrosis. These findings indicate a synergistic effect, where triamcinolone's anti-inflammatory and antiproliferative properties complement BoNT-A's ability to reduce mechanical tension and modulate fibroblast activity. This synergy is supported by Chen & Li et al. [15], who reported that combined triamcinolone and BoNT-A treatment significantly inhibited fibroblast proliferation compared to either monotherapy. The reduced side effects, such as minimal tissue degeneration and necrosis, suggest that combining these agents may mitigate the adverse effects associated with high-dose corticosteroid use, as noted by Zhuang et al. [9].

The superior outcomes in Group D highlight the potential of combination therapy as a multimodal approach to hypertrophic scar management. This aligns with current trends in scar treatment, where multimodal strategies are increasingly favored to address the complex

pathophysiology of hypertrophic scarring [6,16].

The combination of triamcinolone and BoNT-A appears to target multiple aspects of scar formation, including inflammation, fibroblast activity, and mechanical tension, offering a more comprehensive therapeutic effect.

Limitations

This study has some limitations. First, the use of an animal model may not fully replicate the complex wound healing processes in humans. Second, the relatively short follow-up period of four weeks might not adequately reflect long-term scar remodeling and recurrence rates.

CONCLUSION

We conclusion that while intralesional triamcinolone and BoNT-A are each effective in attenuating hypertrophic scar characteristics, their combination produced superior results, with improved tissue reconstruction, reduced inflammation, and fewer adverse effects. These findings highlight the potential of combined therapy as a promising multimodal approach for hypertrophic scar management, particularly in post-surgical, burn, and trauma-related scars. Importantly, this work contributes novel experimental evidence supporting the integration of combination therapy into future clinical practice guidelines.

Conflict of Interest: There are no conflicting interests, according to the authors.

Financial Disclosures: No specific grant from a public, private, or nonprofit funding organization was awarded for this study.

Availability of the data: Upon reasonable request, the associated author will make the datasets created and/or examined during the current work available.

Authors contribution: In addition to writing and getting the book ready for publication, the writers were in charge of gathering and analyzing the data. The final version was examined and approved by all authors.

REFERENCES

1. Chiang RS, Borovikova AA, King K, Banyard DA, Lalezari S, Toranto JD, et al. Current concepts related to hypertrophic scarring in burn injuries. *Wound Repair Regen*. 2016;24(3):466-77. https://doi.org/10.1111/wrr.12432

2. Trisliana PA, Torresetti M, Grassetti L, Nicoli F, Zhang YX, Dashti T, et al. Intralesional injection treatment of hypertrophic scars and keloids: a systematic review regarding outcomes. *Burns Trauma*. 2015;3:14. https://doi.org/10.1186/s41038-015-0015-7

3. Morelli CM, Salzillo R, Segreto F, Persichetti P. Triamcinolone acetonide intralesional injection for the treatment of keloid scars: patient selection and perspectives. *Clin Cosmet Investig Dermatol*. 2018;11:387-96. https://doi.org/10.2147/CCID.S133672

4. Xiao Z, Zhang M, Liu Y, Ren L. Botulinum toxin type A inhibits connective tissue growth factor expression in fibroblasts derived from hypertrophic scar. *Aesthetic Plast Surg*. 2011;35(5):802-7. https://doi.org/10.1007/s00266-011-9690-3

5. Suvarna SK, Layton C, Bancroft JD. Fixation of tissues. In: Suvarna SK, Layton C, Bancroft JD, editors. *Bancroft's theory and practice of histological techniques*. 7th ed. Churchill Livingstone Elsevier; 2013. p. 57-73.

6. Ogawa R, Dohi T, Tosa M, Aoki M, Akaishi S. The latest strategy for keloid and hypertrophic scar prevention and treatment: the Nippon Medical School (NMS) protocol. *J Nippon Med Sch*. 2021;88(1):2-9. https://doi.org/10.1272/jnms.JNMS.2021_88-106

7. Kelly AP. Medical and surgical therapies for keloids. *Dermatol Ther*. 2004;17(2):212-8. https://doi.org/10.1111/j.1396-0296.2004.04022.x

8. Nischwitz SP, Rauch K, Luze H, Hofmann E, Draschl A, Kotzbeck P, et al. Evidence-based therapy in hypertrophic scars: an update of a systematic review. *Wound Repair Regen*. 2020;28(5):656-65. https://doi.org/10.1111/wrr.12839

9. Zhuang Z, Li Y, Wei X. The safety and efficacy of intralesional triamcinolone acetonide for keloids and hypertrophic scars: a systematic review and meta-analysis. *Burns*. 2021;47(5):987-98. https://doi.org/10.1016/j.burns.2021.02.013

10. Zhibo X, Miaobo Z. Botulinum toxin type A affects cell cycle distribution of fibroblasts derived from hypertrophic scar. *J Plast Reconstr Aesthet Surg*. 2008;61(9):1128-9. https://doi.org/10.1016/j.bjps.2008.05.003

11. Xiao Z, Zhang F, Cui Z. Treatment of hypertrophic scars with intralesional botulinum toxin type A injections: a preliminary

report. *Aesthetic Plast Surg*. 2009;33(3):409-12. https://doi.org/10.1007/s00266-009-9334-z

12. Jeong HS, Lee BH, Sung HM, Park SY, Ahn DK, Jung MS, et al. Effect of botulinum toxin type A on differentiation of fibroblasts derived from scar tissue. *Plast Reconstr Surg*. 2015;136(2):171e-8e. https://doi.org/10.1097/PRS.0000000000001438

13. Kim YS, Lee HJ, Cho SH, Lee JD, Kim HS. Early postoperative treatment of thyroidectomy scars using botulinum toxin: a split-scar, double-blind randomized controlled trial. *Wound Repair Regen*. 2014;22(5):605-12. https://doi.org/10.1111/wrr.12204

14. Zelken J, Yang SY, Chang CS, Chang CJ, Yang JY, Chuang SS, et al. Donor site aesthetic enhancement with preoperative botulinum toxin in forehead flap nasal reconstruction. *Ann Plast Surg*. 2016;77(5):535-8. https://doi.org/10.1097/SAP.0000000000000625

15. Chen S, Li Y. Comparison of steroid and botulinum toxin type A monotherapy with combination therapy for treating human hypertrophic scars in an animal model. *Plast Reconstr Surg*. 2018;141(3):451e-2e. https://doi.org/10.1097/PRS.0000000000003426

16. Waibel JS, Wulkan AJ, Shumaker PR. Treatment of hypertrophic scars using laser and laser assisted corticosteroid delivery. *Lasers Surg Med*. 2013;45(3):135-40. https://doi.org/10.1002/lsm.22120

Citation

Anany, R., Mohamed Ahmed Elayady, M., Ali, A. Comparison of Steroid and Botulinum Toxin Type A Monotherapy with Combination Therapy for Human Hypertrophic Scars in an Animal Model. *Zagazig University Medical Journal*, 2025; (5450-5461): -. doi: 10.21608/zumj.2025.417993.4133